

Short communication

A simple route to high performance nanometric metallic materials for Li-ion batteries involving the use of cellulose: The case of Sb

Álvaro Caballero, Julián Morales, Luis Sánchez*

Departamento de Química Inorgánica e Ingeniería Química, Facultad de Ciencias, Campus de Rabanales, Edificio Marie Curie, Universidad de Córdoba, 14071 Córdoba, Spain

Received 24 July 2007; received in revised form 27 September 2007; accepted 29 September 2007

Available online 6 October 2007

Abstract

A facile method for obtaining nanometric Sb particles that perform well as electrode in lithium cells is proposed. The method involves reducing SbCl_3 with NaBH_4 in solution and in the presence of commercial cellulose fibers. Once dry, the resulting composite requires no additive for use in lithium cells, where it delivers high capacity values (*ca.* 470 mAh g^{-1}) after the first few cycles. We believe that cellulose acts as a buffer alleviating the mechanical stress to which the element is subject during the lithium insertion/de-insertion process. In fact, an electrode made from nanometric Sb prepared in the absence of cellulose was found to perform poorly; thus the capacity delivered after the fifteenth cycle was below 100 mAh g^{-1} . © 2007 Elsevier B.V. All rights reserved.

Keywords: Antimony; Nanoparticles; Cellulose; Lithium batteries

1. Introduction

New designs of lithium-ion batteries are being made necessary by the increasing demand for energy density of power supply as new, increasingly powerful portable electronics are emerging. Developing higher energy Li-ion battery electrode materials is therefore a necessity. So far, research in this area has focused on Si, Sn and Sb-based materials which alloy reversibly with Li. Based on their high specific capacity, such materials have been proposed as candidates to replace the conventional graphite negative electrode [1]. However, their high capacities are accompanied by huge volume changes (up to 300%) upon alloying with lithium which can result in dramatic losses of capacity and detract from long-term cycling performance [2].

Most research efforts at alleviating this problem have aimed at reducing particle size in the Li^+ storage material. The shortening of the displacement distance for lithium ions can facilitate their diffusion in the sample improving the rate capability of the compound [3]. Moreover, increasing the electrode surface can also increase the reactivity towards lithium, and therefore the increase of the cell capacity. However, these advantages can be

negligible if this increased reactivity is translated to the electrolyte decomposition, thus degrading the cell performance. In this context, recent studies have shown that reducing particle size does not suffice to ensure a consistently good electrochemical response from a lithium-alloy metal electrode during cycling [4]. Moreover, a simple test has exposed the relative importance of nanosized electrodes. Thus, a standard negative electrode prepared with commercially available nanometric elements (e.g. 50 nm Si from Aldrich) exhibits a rapid decline in specific capacity after each charge–discharge cycle. Therefore, research into anode materials should go beyond the mere preparation of nanometric particles. Once material volume expansion is reduced to the nanodomain by decreasing particle size, the next step should be confining particles separately. In this way, contact between intermetallic particles while growing will be hindered and the formation of cracks in the electrode avoided. One way of reducing metal volume changes and buffering the mechanical stress arising in the lithium alloying/de-alloying process is by embedding the metal nanoparticle into a matrix in order to construct a composite electrode. In this respect, Sony Corporation has recently released Li-ion cells using nanostructured Sn–Co–C negative electrodes [5].

A new approach to the problem has recently been proposed by Dahn and co-workers [6] involving the use of new binders to enhance the electrochemical performance of metallic anode

* Corresponding author. Tel.: +34 957 218620; fax: +34 957 218621.
E-mail address: luis-sanchez@uco.es (L. Sánchez).

materials. These authors obtained excellent performance from a cell made with micrometric silicon simply by replacing the standard binder (PVDF) with sodium carboxymethyl cellulose. Therefore, in the presence of appropriate additives, particle size effects are negligible.

We recently found the *in situ* preparation of tin nanoparticles onto cellulose fibers [7] to provide an excellent method for improving the cyclability of this element in lithium cells. In this work, we extended our method to Sb, an element which has attracted considerable attention by virtue of its high specific capacity (660 A h kg^{-1}) but has poor cycling properties. The alternative approach involving the use of Sb-based intermetallic compounds (*viz.* MSb_x with $1 < x < 3$ and $M = \text{Ti, Mn, Fe, Co, Ni, Cu, Zn}$) instead of the pure element has proved ineffective as well. In fact, these compounds exhibit two main drawbacks, namely: (i) the decline in capacity on cycling is still significant (only nanosized compounds perform well on extended cycling [8,9]); and (ii) more than 50% of the theoretical capacity (relative to pure Sb) is lost by effect of the electrochemical inactivity of the transition metal. Similar results have been obtained with Sb-based oxides. Recently, Sb electrodes of a high electrochemical performance were obtained by two different research groups [10,11]. In both cases, Sb was prepared as nanoparticles either encapsulated by pyrolytic polyacrylonitrile [10] or electrodeposited on Sb_2O_3 [11]. Our method is the simplest of all, however. Thus, Sb nanoparticles are deposited onto cellulose by chemical reduction of SbCl_3 with KBH_4 at ambient temperature for a very short time. The electrochemical response of the resulting Sb-composite electrodes includes a high coulombic efficiency and sustainable high capacity values on prolonged cycling.

2. Experimental

All chemicals used in this work were analytical grade. Antimony nanoparticles were synthesized as follows: an amount of 200 mg of cellulose fibers (Arbocel[®]) was added to a solution containing 1.0 g of SbCl_3 dissolved in 2 mL of 6 M HCl under continuous stirring for 30 min to ensure thorough soaking of the fibers. Then, 4.0 mL of 4 M KBH_4 was added dropwise, the cellulose fibers rapidly acquiring a grey color. After stirring for 10 min, the emulsion was filtered and washed with distilled water and ethanol several times. In order to avoid exposure to air, the composite was soaked with ethanol prior to drying in a vacuum oven at 60°C for 3 h.

X-ray powder diffraction (XRD) patterns were recorded on a Siemens D5000 X-ray diffractometer, using $\text{Cu K}\alpha$ radiation and a graphite monochromator. SEM and HRTEM images were obtained with a JEOL 6400 and a JEOL 2010 microscope, respectively. Electrochemical measurements were performed in two-electrode swagelok-type cells, using lithium as a counter-electrode. The electrolyte was Merck battery electrolyte LP 40 (EC:DEC = 1:1 (w/w), 1 M LiPF_6) containing vinyl carbonate (VC) as additive (2% by weight). Electrode pellets were prepared by pressing, in a stainless steel grid, *ca.* 3 mg of synthesized composite. Galvanostatic tests were conducted under a C/6, C/3 and C galvanostatic regimes (C being defined as 1 Li^+ exchanged in

1 h). Step potential curves were recorded at $2.5 \text{ mV}/0.22 \text{ h}$ per step. Both types of electrochemical measurements were controlled via a MacPile II potentiostat–galvanostat. Impedance measurements from 0.01 to 25 kHz (amplitude 3 mV) were made with a Solartron 1470 battery test unit coupled with a Schlumberger SI 1255 frequency response analyzer.

3. Results and discussion

Fig. 1 shows the X-ray diffraction (XRD) pattern for the Sb–cellulose fiber composite. The pattern was indexed in the rhombohedral system, consistent with Sb (ICDD card no. 35-732). The relative intensity of the (0 1 2) reflection was higher than expected, indicating preferential growth along this direction.

The Sb-containing sample consisted of cross-linked cellulose fibers covered with antimony particles. Fig. 2 shows selected electron micrographs of isolated cellulose fibers following deposition of Sb. The metal particles appear as agglomerates onto cellulose fibers (Fig. 2A); however, they also emerge from them in special forms resembling clouds of particles (Fig. 2B). A more detailed view of the morphology of the Sb-composite is provided by the transmission images (Fig. 2C). Thus, two different groups of particles attached to fibers are observed, namely: (i) highly porous agglomerates of interconnected particles the bounds of which can extend several hundreds of nanometers from the fibers and (ii) close packing of particles along the fibers (see inset of Fig. 2C). This peculiar particle growth pattern is a result of the synthetic procedure. Thus, once the cellulose fibers are soaked in the solution, Sb particles are nucleated from the fiber surfaces. The more solid hypothesis accounting for the formation of porous agglomerates involves the release of hydrogen (a by-product of the chemical reaction). Particle size was in the range 20–40 nm, irrespective of the distance from the fiber surface. In contrast to the tin–cellulose system [7], the presence of organic fibers seems to have no significant influence on particle size. Thus, nanometric Sb particles (60–100 nm) were also obtained by direct reduction of a SbCl_3 solution in the absence of cellulose (Fig. 2D). Fig. 3 shows high-resolution electron micrographs of

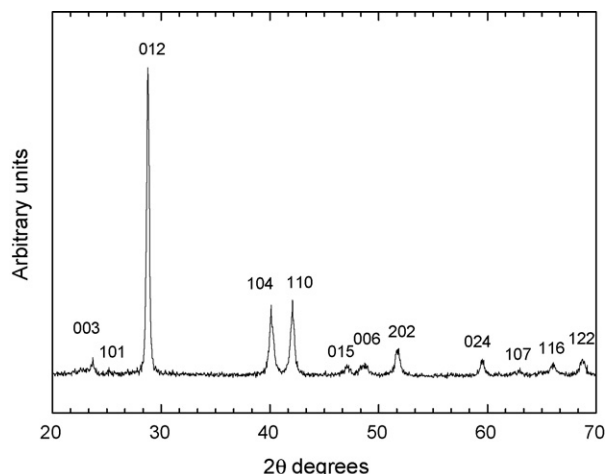


Fig. 1. XRD patterns for the Sb–cellulose composite.

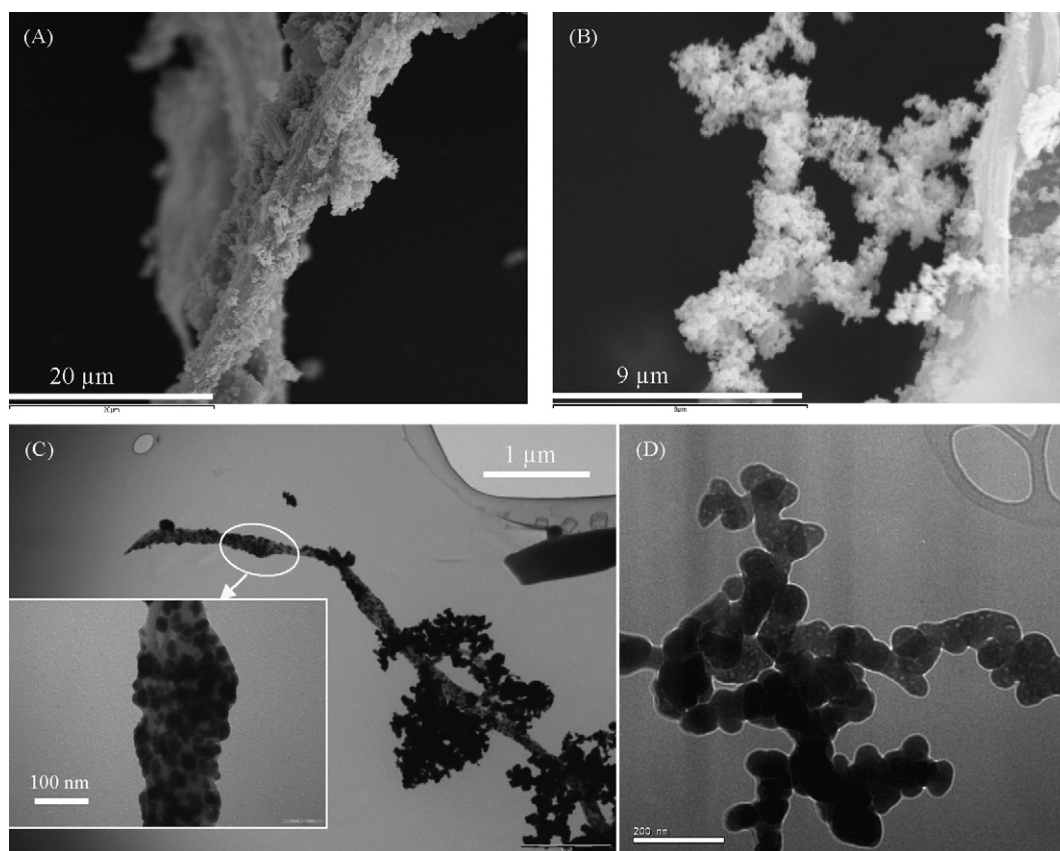


Fig. 2. Sb–cellulose composite: SEM (A and B) and TEM (C) images. (D) TEM image obtained from Sb particles prepared in the absence of cellulose.

an antimony nanoparticle. The lattice fringes reflect the crystalline nature of the Sb nanoparticles. The interplanar spacing was *ca.* 0.31 nm, which is consistent with the (0 1 2) plane.

The electrochemical response of the sample thus prepared was measured in a two-electrode Li/LiPF₆ EC-DEC (2% VC)/Sb–cellulose cell. The amount of Sb was determined from the weight of composite by subtracting the amount of cellulose as evaluated from elemental analysis measurements. The Sb content thus calculated was 61% by weight. The working electrode

contained no electronic conductor or binder additives such as carbon black or PTFE. The open circuit potential of the cell was 2.75 V, which is similar to that reported for Sb-encapsulated electrodes [11]. The cell was cycled over the voltage range 1.5–0.5 V. The first three cycles are shown in Fig. 4a. An abrupt potential drop was observed for the first discharge, followed by an extended plateau at *ca.* 0.8 which can be assigned to the electrochemical formation of Li_xSb alloys occurring as a multi-stage process. The capacity value, 700 mAh g⁻¹, was slightly higher than that corresponding to the formation of a Li₃Sb phase (theoretical capacity 660 mAh g⁻¹). The presence of a coating layer of Sb₂O₃, undetected by XRD, might be responsible for this difference. In fact, there is a small lithium uptake at the beginning of the discharge process which can be tentatively assigned to a Sb³⁺/Sb reduction process [12,13]. On charging the cell, an extended plateau was observed at *ca.* 1.1 that we assigned to a dealloying process. However, not all lithium inserted was removed, so the irreversible slightly exceeded 150 mAh g⁻¹. This value decreased markedly over the next cycles; also, the coulombic efficiency approached 99%, consistent with reversibility in the Li/Sb–cellulose system.

To shed some light on the lithium insertion/deinsertion mechanism, step potential curves were recorded for Li/LiPF₆ EC-DEC (2% VC)/Sb–cellulose cell cycled over the 1.5–0.5 V range, Fig. 4b. The strong and broad peak at *ca.* 0.7 V is consistent with the extended plateau observed in the galvanostatic curve at 0.8 V. Its origin is mainly due to the alloy formation that

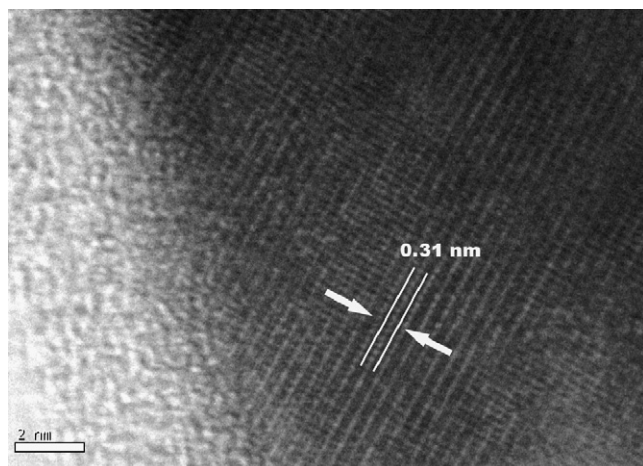


Fig. 3. HRTEM images of Sb nanoparticles.

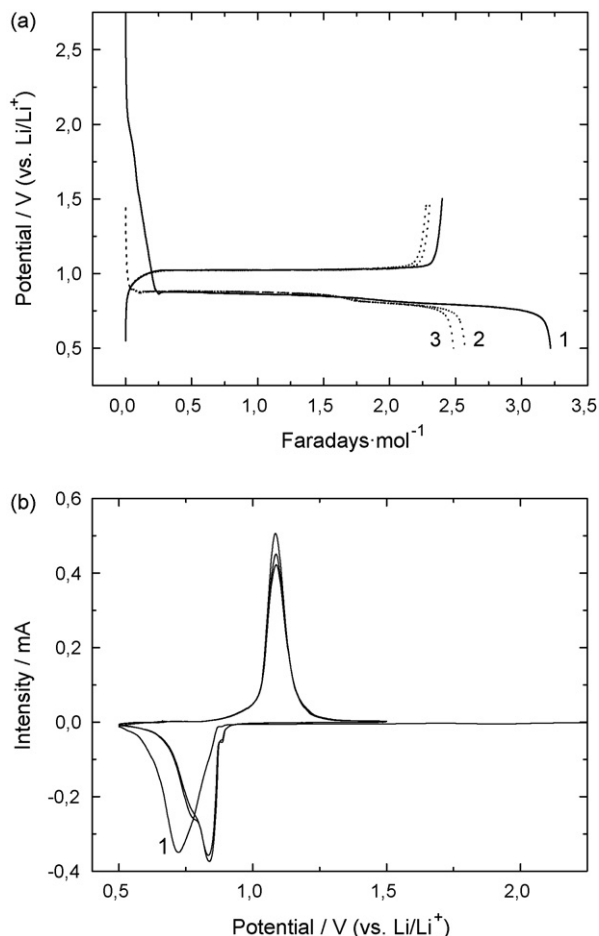


Fig. 4. (a) First three galvanostatic discharge–charges curves, recorded at C/6, and (b) step potential curves for Li/Sb–cellulose cell.

takes place as suggests the peak broadening. The peak asymmetry also reveals that secondary reactions (such as electrolyte reduction and the subsequent formation of a solid electrolyte interface) can occur. Two peaks at 0.84 and 0.78 V were repeatedly observed in the subsequent cycles, which can be ascribed to the $\text{Sb} \rightarrow \text{Li}_2\text{Sb}$ and $\text{Li}_2\text{Sb} \rightarrow \text{Li}_3\text{Sb}$ electrochemical processes, respectively [14]. On charging the cell, a strong, symmetric and narrower peak is observed. This peak at about 1.1 V is assigned to de-alloying process. Apart from the above commented electrochemical process, no other signals were observed, which exclude the participation of cellulose as electrochemical active material, also confirmed by using pure cellulose as electrode.

Fig. 5a shows the variation of the specific capacity of the Li/LiPF₆ EC-DEC (2% VC)/Sb–cellulose cell with the number of cycles. An average value of 470 mAh g⁻¹ (specific capacity referred to that of Sb in the composite) was nearly maintained on cycling at C/6. Even though a slight decline of capacity was observed on cycling, the capacity retention can be considered quite good compared with the electrode made from pure Sb nanoparticles obtained in the absence of cellulose by using the same procedure. In this case, the capacity faded abruptly (below 100 mAh g⁻¹ at the fifteenth cycle). Therefore, simply using nanometric particles does not ensure good performance of the resulting cell probably because mechanical stress induced by

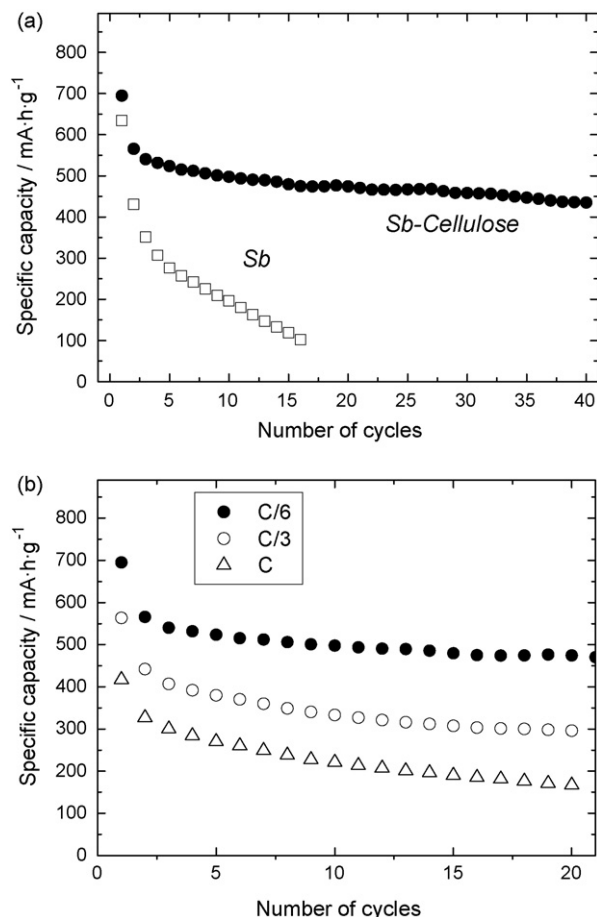


Fig. 5. (a) Specific discharge capacity delivered by the Li/Sb–cellulose and Li/Sb cells upon cycling at C/6 regime. (b) Specific discharge capacity delivered by the Li/Sb–cellulose cell at different cycling rates.

volume changes upon alloying/de-alloying persists. By contrast, the special morphology of the composite electrode facilitates absorption of the volume expansions and contractions occurring during Li insertion and de-insertion. Although mechanical stress is mainly buffered by the cellulose fibers, one cannot exclude a favourable effect of the highly porous system created by this synthetic procedure.

Cell performance is similar to that reported by He et al. [11]; however, their method involves heating at 300 °C under N₂ to pyrolyse the polymer. Although capacity values reported by Bryngelsson et al. [10] were somewhat higher (*ca.* 600 mAh g⁻¹), they were obtained for an Sb/Sb₂O₃ electrode where the contribution of Sb₂O₃ to the capacity was not quantified; also, the amount of Sb deposited was too small (*ca.* 0.1 mg cm⁻²), and these authors adopted the criterion of depositing onto a large area and assuming uniform electrodeposition. We believe better accuracy in the active amount used would be required in order to establish a more rigorous comparison.

Even though the cellulose is an insulating material, the conductivity properties of composite electrode must be quite good as revealed by the electrochemical response of electrode (in fact, it was unnecessary to add any carbon black to make electrochemical measurements). Thus, the electron motion during the successive charge–discharge processes would be assured by

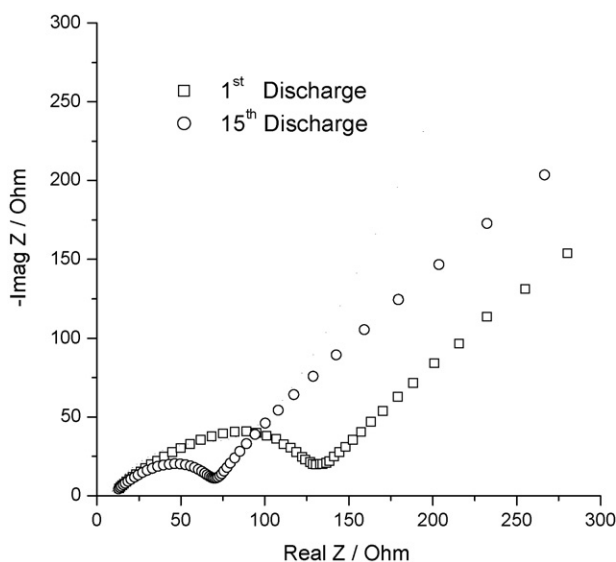


Fig. 6. Impedance spectra for Sb–cellulose electrode in the discharged state at 0.5 V after the first and fiftieth cycle.

assuming a good contact between the Sb nanoparticles that coat the cellulose fiber surface and, also, between the particles and the stainless steel grid collector [7]. The role played by cellulose on the Li^+ ion diffusion is unknown, but it is not detrimental for this property. Recently, Pushparaj et al. [15] have developed a very innovative anode material consisting of graphite nanotubes immersed on a cellulose matrix, acting as the electrolyte support. This performance gives additional support on the beneficial role played by the cellulose in the field of Li-ion batteries. The composite electrode has the ability to deliver good capacities at higher rates (see Fig. 5b). As commonly observed, the capacity faded by increasing the rate capability, but the decrease was moderated and, quite relevant, the capacity retention was somewhat similar to that observed at the lowest rate tested (C/6).

Additional information for understanding the electrochemical behavior of the composite electrode was obtained from impedance measurements. Fig. 6 shows the Nyquist plots of Sb–cellulose electrode discharged at 0.5 V for the first and fiftieth cycle. The broad shape of semi-circle is characteristic with the presence of two kinds of resistance due to: (i) the formation of passivation film on the surface (SEI film), at higher frequencies, and (ii) the Li^+ charge transfer at interface, at middle frequency region. The impedance significantly decreased on cycling. This behavior has been associated to the pulverization of metallic particles [16] and is consistent with that reported for Sb intermetallic alloys that have also good capacity retentions [16]. The slope of straight line at low frequency corresponds to the Li-

ion diffusion in the bulk material. Its value hardly changed with cycling, indicative that the lithium mobility is maintained.

In summary, the proposed method provides a simple, one-step chemical reduction procedure affording the effective preparation of highly crystalline Sb nanoparticles onto cellulose fibers. The morphology of the resulting Sb-composite is special: metal particles deposit onto the organic fibers and form highly porous agglomerates around them. This system acts as a good electrode material for lithium cells which exhibit very good electrochemical performance without the need for any additives. Thus, the Li/LiPF₆ EC-DEC (2% VC)/Sb–cellulose cell delivers capacities above 470 mAh g⁻¹ on prolonged cycling. Also, its electrochemical behavior surpasses that of nanoparticulate Sb prepared in the absence of cellulose. Therefore, cellulose is a powerful binder for preparing efficient metal–composite anode materials for Li-ion batteries [7].

Acknowledgements

This work was supported by CICyT (MAT2005-03069) and Junta de Andalucía (Group FQM 175).

References

- [1] Y. Idota, T. Kubota, A. Matsufuji, Y. Maekawa, T. Misayaka, *Science* 276 (1997) 1395.
- [2] L.Y. Beaulieu, K.W. Eberman, R.L. Turner, L.J. Krause, J.R. Dahn, *Electrochim. Solid-State Lett.* 4 (2001) A137.
- [3] Y. Xia, M. Yoshio, H. Noguchi, *Electrochim. Acta* 52 (2006) 240.
- [4] M.N. Obrovac, L.J. Krause, *J. Electrochem. Soc.* 154 (2007) A103.
- [5] H. Inoue, Communication no. 228 Proceedings of International Meeting on Lithium Batteries, Biarritz, France, June 18–23, 2006.
- [6] J. Li, R.B. Lewis, J.R. Dahn, *Electrochim. Solid-State Lett.* 10 (2007) A17.
- [7] A. Caballero, J. Morales, L. Sánchez, *Electrochim. Solid-State Lett.* 8 (2005) A464.
- [8] J. Ren, X. He, W. Pu, C. Jiang, C. Wan, *Electrochim. Acta* 52 (2006) 1538.
- [9] J. Xie, G.S. Cao, X.B. Zhao, Y.D. Zhong, M.J. Zhao, *J. Electrochem. Soc.* 151 (2004) A1905.
- [10] H. Bryngelsson, J. Eskhult, L. Nyholm, M. Herranen, O. Alm, K. Edström, *Chem. Mater.* 19 (2007) 1170.
- [11] X. He, W. Pu, L. Wan, J. Ren, C. Jiang, C. Wan, *Electrochim. Acta* 52 (2007) 3651.
- [12] H. Li, X. Huang, L. Chen, *Solid State Ionics* 123 (1999) 189.
- [13] J. Santos, J. Cuart, A. Caballero, J. Morales, L. Sánchez, *J. Solid State Chem.* 177 (2004) 2920.
- [14] C.-M. Park, S. Yoon, S.-I. Lee, J.-H. Kim, J.-H. Jung, H.-J. Sohn, *J. Electrochem. Soc.* 154 (2007) A917.
- [15] V.L. Pushparaj, M.M. Shaijumon, A. Kumar, S. Murugesan, L. Ci, R. Vajtai, R.J. Linhardt, O. Nalamasu, P.M. Ajayan, *Proc. Natl. Acad. Sci. U.S.A.* 104 (2007) 13574.
- [16] H. Zhao, C. Yin, H. Guo, W. Qiu, *Electrochim. Solid-State Lett.* 9 (2006) A281.